IMPROVED MEASUREMENT OF THE KINETICS OF CRYSTALLIZATION IN A BATCH EXPERIMENT

Jaroslav NÝVLT and Miloslav KAREL

Institute of Inorganic Chemistry,
Academy of Sciences of the Czech Republic, 160 00 Prague 6, The Czech Republic

Received August 13, 1992
Accepted October 17, 1992

An improved method is described whereby knowledge of the supersaturation course during a run and measurement of the final product crystal size distribution yield the growth rate of crystals and the nucleation rate in a wide range of supersaturations from only a single batch experiment. The evaluation method is refined by the interpolation of experimental data for short intervals of time. The method is illustrated using potassium sulfate crystallization as an example.

Design-oriented kinetic data of crystallization are frequently obtained from continuous MSMPR (Mixed Suspension–Mixed Product Removal) crystallizer experiments[1]. Although batch experiments are usually simpler than continuous ones, they involve more complicated evaluation of data. In this paper, we shall briefly describe an improved method, which starts with the knowledge of the supersaturation course during the run and of the final product crystal size distribution, and yields both the growth rate and nucleation rate of crystals in the full range of achievable supersaturation.

THEORETICAL

The batch experiment is very simple: it starts with a solution heated to slightly above the saturation temperature T_{eq}, cooled down to a little below this temperature, seeded with a few crystals in order to control the metastable zone width, and then cooled down to the final temperature T_f. Either at short time intervals or continuously, the temperature and concentration of the solution are measured. The concentration can be monitored by refractometry, densitometry, conductometry or by other methods. After reaching T_f, the suspension is stirred until a steady state has been established and the product crystals' size distribution is determined.

The supersaturation is calculated from measured conductivity data using two fixed points for interpolation: the equilibrium conductivities of the saturated solution close to 60 or close to 50 °C and of the suspension in equilibrium at the end of the experiment. Measurements carried out at different temperatures show that linear interpolation is sufficient in the case of K_2SO_4 solutions within this limited temperature range.

Thus, from a batch experiment there results a series of data time t–temperature T–supersaturation Δw. The final crystal size distribution $M(L)$ (oversize fraction) can be described by the well known equation[2]

$$M(L) = 100\,(1 + z + z^2/2 + z^3/6)\exp(-z) \qquad (1)$$

with

$$z = 3\,(L - L_N)/\dot{L}t_c\,, \qquad (2)$$

where $3/(\dot{L}t_c)$ is the slope of the lines in a z–L diagram of the corresponding crystal size distribution.

The total mass of crystals m_c is given by the mass balance[3]

$$m_c = m_0\,(w_0 - w_f)\,, \qquad (3)$$

where m_0 is total mass of H_2O in the batch and w_0, w_f are the corresponding initial and final concentrations, respectively. Knowing the mass of crystals and their average size, we can calculate their total number[2]:

$$N_c = \frac{2\,m_c}{9\,\alpha\,\rho_c\,L_{mean}^3}\,. \qquad (4)$$

The product can now be subdivided into a large number (i.e. several hundreds or several thousands, depending on the duration of the experiment) of fractions, k, according to crystal size. Denoting the width of each fraction as ΔL, we can obtain the number of crystals in each fraction and their mass[4]:

$$N_{c,i} = N_c\,[\exp(-z_1) - \exp(-z_2)]\,, \qquad (5)$$

where

$$z_1 = 3\,(L_i - L_N)/\dot{L}t_c\,, \qquad z_2 = 3\,(L_i - L_N + \Delta L)/\dot{L}t_c\,. \qquad (6)$$

For each crystal size, the mass balance must be

$$m_{c,i} = \alpha \rho_c N_{c,i} L_i^3 \tag{7}$$

$$m_{c,tot} = \sum_i^k m_{c,i} . \tag{8}$$

Thus, in the next step, starting from the end of the experiment, a size decrease $(L_{i,t-1} - L_{i,t})$ is sought for each instant that would give the correct mass of product crystals[4] corresponding to the mass balance

$$m_{c,t} = m_0 (w_0 - w_t) = m_{c,tot,t} . \tag{9}$$

The concentration at a given instant is calculated by interpolation; the intervals must be small enough to correspond to the calculated number of crystal fractions. Interpolation at one-minute intervals is reasonably sufficient in our case. The crystal growth rate is then

$$\dot{L}_t = \frac{L_{i,t-1} - L_{i,t}}{\Delta t} \tag{10}$$

and the nucleation rate

$$\dot{N}_{N,t} = \frac{N_{c,t-1} - N_{c,t}}{m_0 \Delta t} , \tag{11}$$

where the difference in the number of crystals is given by the disappearance of fractions when $L_{i,t-1} \leq 0$.

The dependencies $\dot{L}(\Delta w)$ and $\dot{N}_N(\Delta w)$ can then be expressed by the power laws[2]

$$\dot{L} = k_G \Delta w^g$$

$$\dot{N}_N = k_N \Delta w^n . \tag{12}$$

However, the temperature dependence of $\dot{L}$ must be taken into account[4], because our data from a cooling batch experiment are polythermal. From the theory of crystal growth[4] it may be presumed that

$$\frac{d \ln \dot{L}}{d \ln \Delta w} \cong 0.5 . \tag{13}$$

EXPERIMENTAL

The apparatus is identical to that described in the previous paper[4]. It consists of a jacketted glass crystallizer with a two-blade stirrer and one baffle. The temperature in the crystallizer is controlled by a thermostat containing a resistance thermometer. This thermostat in turn is controlled by a temperature programmer which sets the initial temperature and the required cooling rate down to the final temperature T_f. The temperature in the crystallizer is measured using a resistance thermometer, connected to a bridge. Its output signal is led to a digital meter and a registering device. In our experiments, the concentration is measured continuously using a home-made conductometer designed for concentrated electrolyte solutions[5]. Its output signal again is read using a digital meter and a line recorder.

Experiments starting with K_2SO_4 aqueous solutions cooled down from 60 to 30 °C can serve as an example. Four experiments with parameters given in Table I have been carried out.

TABLE I
Parameters of individual experiments

Experiment No.	T_0, °C	T_{eq}, °C	T_f, °C	w_0, kg/kg$_{H_2O}$	t_c, min
1	55.45	49.90	29.99	0.166	160
2	64.0	60.0	29.77	0.183	260
3	64.5	60.0	32.4	0.183	365
4	66.0	60.0	32.97	0.183	380

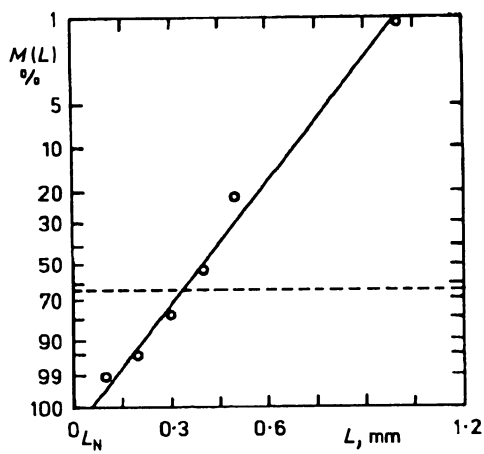

FIG. 1
Size distribution of product crystals from experiment No. 1 shown in a z–L plot

RESULTS AND DISCUSSION

In all of the experiments, the product crystal size distribution (Table II) was evaluated using the method of least squares applied to the Eq. (*1*). The linearized z–L plot of the crystal size distribution of the product from experiment No. 1, shown in Fig. 1, may serve as an example. This plot is based on Eq. (*1*): using an iterative method, values of the dimensionless crystal size z have been calculated from experimental oversize fractions $M(L)$ and these values of z have then been plotted against the corresponding crystal sizes L; the $M(L)$ scale is again calculated from Eq. (*1*). The plot of the supersaturation obtained in this experiment is presented in Fig. 2. In the beginning, the supersaturation increases at an almost constant rate; when nucleation starts and precipitation leads to a decrease in concentration, the supersaturation decreases exponentially. So rising supersaturation leads to nucleation, whereas the decreasing part yields the growth rate. Corresponding plots from all the experiments are similar in character. The calculated slopes of the crystal size distribution plots, as well as those of maximum supersaturations, maximum crystal growth rates and maximum nucleation rates, are summarized in Table III. The crystal growth rates and nucleation rates as obtained from

TABLE II
Size distribution of product crystals from batch experiments 1 – 4

L_i	1		2		3		4	
	$M(L)$	z	$M(L)$	z	$M(L)$	z	$M(L)$	z
1.2					40.29	4.16	38.57	4.25
1.0	1.12	9.89	18.54	5.65	53.38	3.51	52.03	3.58
0.75			63.45	3.06	66.68	2.91	64.12	3.03
0.6			85.73	2.00	80.55	2.27	77.50	2.42
0.5	21.99	5.34	92.21	1.59	87.36	1.91	84.62	2.05
0.4	53.82	3.49	97.86	1.04	94.46	1.41	94.29	1.43
0.3	78.54	2.37	98.83	0.86	96.68	1.19	96.84	1.17
0.2	95.47	1.32	99.56	0.65	98.13	0.99	98.41	0.95
0.1	99.25	0.76	99.80	0.52	98.68	0.89	98.90	0.85
0.08			99.89	0.44	98.94	0.84	99.15	0.78
0.075			99.94	0.37	99.23	0.76	99.36	0.72
L_N, mm	0.054		0.11		0		0	
$\bar{L}\,t_1$, mm	0.0939		0.179		0.268		0.262	

the equations listed in the theoretical section are plotted in Figs 3 – 7. Figure 3 shows that the dependence of the linear growth rate on supersaturation is curved so the power is greater than 1. From the logarithmic plot (Fig. 4) it follows that the exponent in the

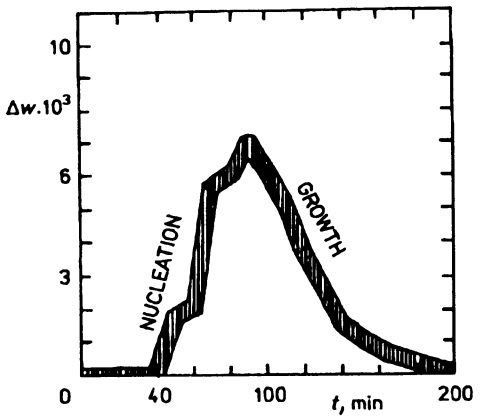

FIG. 2
Supersaturation as a function of time (experiment No. 1). The zone width denotes the probable error

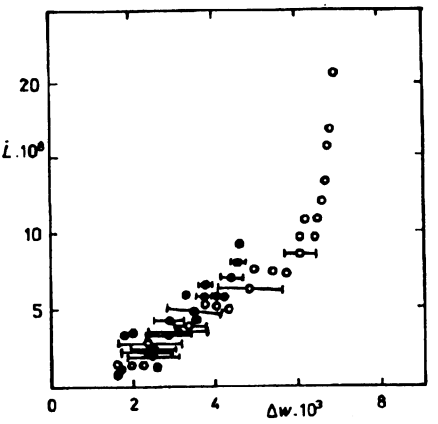

FIG. 3
Linear crystal growth rate as a function of supersaturation. ○ experiment 1, ⊗ expriment 2, ⊖ experiment 3, ⊙ experiment 4. The lines denote the spread of data

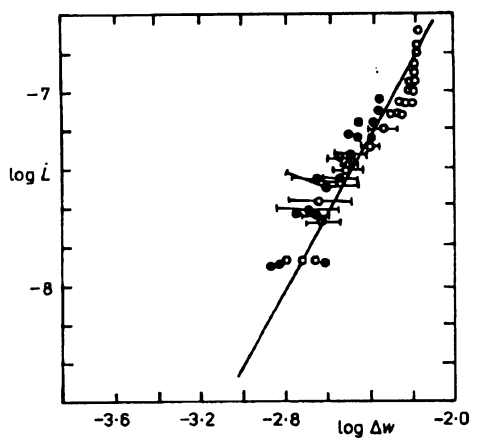

FIG. 4
Linear crystal growth rate as a function of supersaturation (logarithmic scale). Notation of points as in Fig. 3. Full line for $g = 2$

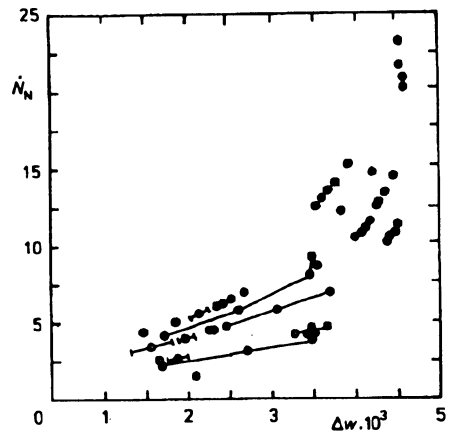

FIG. 5
Nucleation rate as a function of supersaturation. Notation of points as in Fig. 3

power-law Eqs (*12*) is $g \cong 2$. A similar exponential increase with supersaturation shows the nucleation rate (Fig. 5) and from the logarithmic plot (Figs 6, 7) may be found $n \cong 2 - 3$ in the region of low supersaturations and $n \cong 8 - 10$ in the whole space of supersaturations reached in our experiments, which corresponds to the literature[6].

TABLE III
Maximal values in experiments 1 – 4

Parameter	1	2	3	4
$\Delta w \cdot 10^3$	6.975	2.57	3.45	3.66
$\dot{L} \cdot 10^8$	25.6	9.24	4.73	5.69
$\dot{N}_N$	660	22	9	7
T_{max}[a]	41.74	51.62	50.75	53.85

[a] Temperature corresponding to the maximum of supersaturation, of the crystal growth rate and of the nucleation rate.

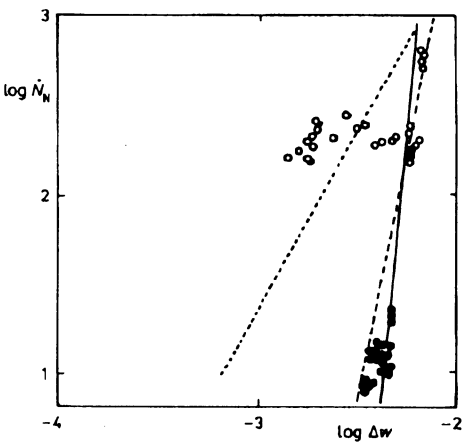

FIG. 6
Nucleation rate as a function of supersaturation (logarithmic scale, all experiments). Notation of points as in Fig. 3. n = 2 (· · · ·), 5 (– – – –), 10 (——)

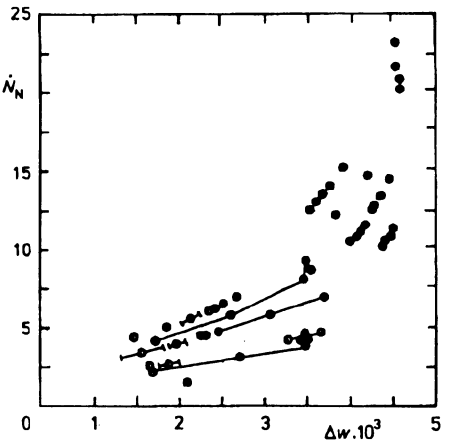

FIG. 7
Nucleation rate as a function of supersaturation (logarithmic scale, experiments with lower supersaturation). Notation of points as in Fig. 3. Full line for n = 2

CONCLUSION

It can be seen from the figures that the growth rate data as well as the nucleation rate data from individual experiments are consistent and that they can be compared with available literature data. Values of the nucleation exponents are lower at low supersaturations, where secondary nucleation due to crystal collisions prevails; at higher supersaturations, high nucleation exponents indicate the prevalence of secondary nucleation through adsorption layer mechanisms.

The reliability of the data is significantly improved using interpolated values of supersaturation with narrower crystal size fractions.

We thus can conclude that the results, in particular for the growth rate, are satisfactory and that it is possible to obtain design oriented kinetic data of crystalization from any batch experiment provided that the supersaturation during the run and the final crystal size distribution are known.

SYMBOLS

g	growth rate order
k	number of fractions
k_G	growth rate constant
k_N	nucleation rate constant
L	crystal size
L_N	initial crystal size
L_{mean}	mean crystal size
ΔL	size increment
$\dot{L}$	linear crystal growth rate
$M(L)$	crystal size distribution
m_0	total mass of solvent
m_c	mass of crystals
$m_{c,tot}$	total mass of crystals at the end of a batch
N_c	number of crystals
$\dot{N}_N$	nucleation rate
n	nucleation exponent
t	time
t_c	batch time
T	temperature
T_{eq}	equilibrium temperature of saturated solution
T_0	initial temperature
T_f	final temperature
w	solution concentration
w_o	initial solution concentration
w_f	concentration of mother liquor
Δw	supersaturation
z	dimensionless crystal size
α	volume shape factor
ρ_c	crystal density

This research has been supported by the Grant Agency of the Academy of Sciences of the Czech Republic, grant No. 43 211.

REFERENCES

1. Randolph A. D., Larson M. A.: *Theory of Particulate Processes*, Chaps 4, 6, 9. Academic Press, New York 1971.
2. Nývlt J., Söhnel O., Matuchová M., Broul M.: *The Kinetics of Industrial Crystallization*, pp. 69, 178, 234. Academia, Prague 1985.
3. Nývlt J., Kočová H.: Chem. Prum. *26*, 567 (1976).
4. Nývlt J.: Collect. Czech. Chem. Commun. *54*, 3187 (1989).
5. Nývlt J., Karel M., Písařík S.: Chem. Prum., in press.
6. Karel M., Nývlt J.: Collect. Czech. Chem. Commun. *58*, 1848 (1993).

Translation revised by I. Kovářová.